

# TENSORIAL COMPRESSIVE SENSING OF JOINTLY SPARSE MATRICES WITH APPLICATIONS TO COLOR IMAGING\*

Edgar A. Bernal

United Technologies Research Center  
bernalea@utrc.utc.com  
411 Silver Ln., East Hartford, CT 06118

Qun Li

Microsoft Corporation  
qul@microsoft.com  
11025 NE 8th St., Bellevue, WA 98004

## ABSTRACT

The tasks of color and hyperspectral image reconstruction have been addressed in the context of Compressive Sensing (CS) frameworks in the past. Traditional CS methodologies exploit the underlying assumption that images are intrinsically sparse in some domain in order to reconstruct the image with few linear measurements, relative to its original dimensionality. Since the different color or spectral planes of such imagery are usually correlated, exploiting joint sparsity principles has been shown to be beneficial. Specifically, images reconstructed from a given number of measurements with so-called Multiple Measurement Vector (MMV) approaches have better fidelity relative to those yielded by Single Measurement Vector (SMV) frameworks which don't exploit joint sparsity constraints. Standard MMV approaches, however, operate by vectorizing the data, and effectively fail to preserve the intrinsic high-dimensional structure of the imagery. In this paper, we introduce a tensorial MMV approach that exploits joint sparsity constraints across both spatial dimensions of the images as opposed to only the rows or columns, as in traditional vectorial approaches, while still leveraging joint sparsity assumptions across the color or spectral planes. We demonstrate empirically that our method provides better reconstruction fidelity given a fixed number of measurements, and that it is also more computationally efficient.

**Index Terms**— Color and hyperspectral imaging, tensorial compressive sensing, joint sparsity, multiple measurement vector

## 1. INTRODUCTION

Compressive Sensing (CS) refers to the reconstruction of sparse signals given a small number of linear measurements, relative to the signal dimensionality. CS can be posed as an optimization problem aiming at finding the solution of an under determined system of equations. A vector  $\mathbf{x} \in \mathbb{R}^N$  is called  $s$ -sparse if it has at most  $s$  non-zero entries. The sampling process consists in obtaining samples  $\mathbf{y} \in \mathbb{R}^m$  via the operation  $\mathbf{y} = \mathbf{A}\mathbf{x}$ , where  $\mathbf{A} \in \mathbb{R}^{m \times N}$  is the sampling matrix

and  $m < N$ . This sampling and recovery process is equivalent to the Single Measurement Vector (SMV) problem. The reconstruction process attempts to recover  $\mathbf{x}$  by finding a solution  $\hat{\mathbf{z}} \in \mathbb{R}^N$  satisfying

$$\hat{\mathbf{z}} = \arg \min_{\mathbf{z}} \|\mathbf{z}\|_0 \quad \text{s.t.} \quad \mathbf{y} = \mathbf{A}\mathbf{z}. \quad (1)$$

This  $\ell_0$  minimization problem is NP-hard, and thus, computationally intractable, so it is often approximated by optimizing the  $\ell_1$  equivalent or by implementing greedy algorithms. According to the Multiple Measurement Vector (MMV) approach, when the signal to be reconstructed comprises a set of  $q$  vectors  $\mathbf{x}_j \in \mathbb{R}^N$  with common support, that is, when  $\mathbf{X} = [\mathbf{x}_1 | \mathbf{x}_2 | \dots | \mathbf{x}_q]$  (in the case of an RGB image,  $\mathbf{x}_j$  for  $1 \leq j \leq q = 3$ , correspond to the vectorized color planes), simultaneous sampling of the vectors takes place so that  $\mathbf{Y} = \mathbf{A}\mathbf{X}$ , where  $\mathbf{Y} = [\mathbf{y}_1 | \mathbf{y}_2 | \dots | \mathbf{y}_q] \in \mathbb{R}^{m \times q}$ . The optimization task in the MMV recovery problem can be formulated as

$$\hat{\mathbf{Z}} = \arg \min_{\mathbf{Z}} \|\mathbf{Z}\|_{2,0} \quad \text{s.t.} \quad \mathbf{Y} = \mathbf{A}\mathbf{Z}, \quad (2)$$

where  $\|\mathbf{Z}\|_{2,0}$  denotes the  $\ell_0$  norm of the vector whose elements are  $\ell_2$  norms of the rows of matrix  $\mathbf{Z}$  [1].

### 1.1. Related Work

Solving the optimization task in Eq. 2 is a (nondeterministic polynomial) NP-hard problem. Various methods have been proposed to address the problem via convex relaxation [1, 2, 3, 4] or approximation [5]. In addition to proposing an optimization-based approach which yields an approximate solution to Eq. 2, the study in [5] also attempted to apply the MMV recovery approach to the problem of reconstructing color images, which had previously been formulated as a group-sparse recovery problem [6, 7]. The direct extension of [5] to hyperspectral image reconstruction (HSI) is trivial. Other solvers to Eq. 2 have been proposed more recently, but they impose a stricter constraint on the MMV problem, where the measurement matrix is not only assumed to be jointly-sparse but also of low rank [8, 9]. Traditional CS theory is well-suited for sampling and reconstruction of one-dimensional signals, and naïve extensions of the CS framework to multidimensional problems typically rely on vectorial

\*This work was done while the authors were with PARC, A Xerox Company

representations of the data, which result in increased computational and memory requirements. Color and hyperspectral images, as well as video streams are intrinsically high-order, and their reconstruction is not adequately addressed by vectorial approaches. The extension of the CS theory to multi-dimensional data with applications in HSI is a research topic that has received increased attention in recent years [10, 11, 12]. However, none of these methods exploits joint sparsity in the spectral or spatial domain, unlike the method proposed in the present paper.

## 1.2. Contributions

In this paper, we propose a non-trivial extension of the approach proposed in [5] which is, to our knowledge, the state-of-the-art with regards to MMV recovery of a signal with jointly sparse components that does not impose additional constraints. Our two main contributions are as follows: firstly, we introduce a tensorial MMV sampling framework, which effectively preserves the spatial nature of each of the planes of the imagery by foregoing the vectorization step in previously proposed MMV approaches for color image sampling and reconstruction [5]; secondly, instead of posing the recovery problem as a row-sparse MMV recovery problem as in [5], which exploits joint sparsity across the color dimension only, we introduce a two-fold row-sparse recovery framework, which exploits the joint sparsity that both rows and columns exhibit across the color dimension. In short, the proposed method leverages the tensorial nature of the data being sampled and reconstructed at both stages of the process, which results in improved reconstruction performance and computational efficiency.

## 2. NOTATION AND TERMINOLOGY

We follow the convention used in [13][10], the relevant portion of which we summarize next for convenience. *Italic* characters represent scalar values (*e.g.*,  $a, B$ ), **bold-face** characters represent vectors (*e.g.*,  $\mathbf{a}, \mathbf{b}$ ), **capital italic bold-face** characters represent matrices (*e.g.*,  $\mathbf{A}, \mathbf{B}$ ) and **capital calligraphic** characters represent tensors (*e.g.*,  $\mathcal{A}, \mathcal{B}$ ). A tensor is a multidimensional array. The order or number of dimensions of a tensor corresponds to its number of modes. For instance, tensor  $\mathcal{X} \in \mathbb{R}^{N_1 \times \dots \times N_d}$  has order  $d$  (or is  $d$ -dimensional), and the dimensionality of its  $i^{\text{th}}$  mode (also denoted mode  $i$ ) is  $N_i$ .

### 2.1. Multilinear Algebra

**Kronecker product** The Kronecker product of matrices  $\mathbf{A} \in \mathbb{R}^{I \times J}$  and  $\mathbf{B} \in \mathbb{R}^{K \times L}$  is denoted by  $\mathbf{A} \otimes \mathbf{B}$ . The result is a matrix of size  $(I \cdot K) \times (J \cdot L)$  defined by  $\mathbf{A} \otimes \mathbf{B} =$

$$\begin{pmatrix} a_{11}\mathbf{B} & a_{12}\mathbf{B} & \cdots & a_{1J}\mathbf{B} \\ a_{21}\mathbf{B} & a_{22}\mathbf{B} & \cdots & a_{2J}\mathbf{B} \\ \vdots & \vdots & \ddots & \vdots \\ a_{I1}\mathbf{B} & a_{I2}\mathbf{B} & \cdots & a_{IJ}\mathbf{B} \end{pmatrix}.$$

**Mode- $i$  fiber and mode- $i$  unfolding** The mode- $i$  fibers of tensor  $\mathcal{X} = [x_{\alpha_1, \dots, \alpha_i, \dots, \alpha_d}] \in \mathbb{R}^{N_1 \times \dots \times N_i \times \dots \times N_d}$  are obtained

by fixing every index but  $\alpha_i$ . The mode- $i$  unfolding of  $\mathcal{X}$ , denoted  $\mathbf{X}_{(i)}$ , equals a matrix of size  $N_i \times (N_1 \dots N_{i-1} \cdot N_{i+1} \dots N_d)$  whose columns are the mode- $i$  fibers of  $\mathcal{X}$ .

**Mode- $i$  product** The mode- $i$  product between tensor  $\mathcal{X} = [x_{\alpha_1, \dots, \alpha_i, \dots, \alpha_d}] \in \mathbb{R}^{N_1 \times \dots \times N_i \times \dots \times N_d}$  and matrix  $\mathbf{U} = [u_{j, \alpha_i}] \in \mathbb{R}^{J \times N_i}$  is a tensor  $\mathcal{X} \times_i \mathbf{U} \in \mathbb{R}^{N_1 \times \dots \times N_{i-1} \times J \times N_{i+1} \times \dots \times N_d}$ , and is defined element-wise as

$$(\mathcal{X} \times_i \mathbf{U})_{\alpha_1, \dots, \alpha_{i-1}, j, \alpha_{i+1}, \dots, \alpha_d} = \sum_{\alpha_i=1}^{N_i} x_{\alpha_1, \dots, \alpha_i, \dots, \alpha_d} u_{j, \alpha_i}.$$

## 3. TENSORIAL COMPRESSIVE SENSING OF JOINTLY SPARSE MATRICES

We propose an extension of the Multiple Measurement Vector (MMV) sampling and recovery approach to tensorial data. In the past, color and hyperspectral image reconstruction in a CS framework was formulated as a group- or row-sparse recovery problem [5]. Similar to most CS methodologies, the proposed approach is implemented in two stages: a sampling and a reconstruction stage. In the *sampling stage*, an imaging device obtains a set of linear measurements from the image of a scene; subsequently, a color representation of the scene is recovered from the measurements in the *reconstruction stage*.

### 3.1. Sampling Stage

We denote the sampled color cube representing the image as a tensor of order three  $\mathcal{X} \in \mathbb{R}^{N_r \times N_c \times N_b}$ , where  $N_r$  and  $N_c$  are the number of rows and columns of the image, respectively, and  $N_b$  is the number of color planes. We refer to the row, column and color/spectral dimensions of the image as modes 1, 2 and 3 of the tensor, respectively. Sampling of  $\mathcal{X}$  is achieved by performing a set of mode- $i$  products between  $\mathcal{X}$  and sampling matrices  $\mathbf{U}_i$ , for  $i = 1, 2$ , one for each spatial tensor mode. The entries of the sampling matrices are randomly generated, for example, drawn from a Gaussian distribution. Without loss of generality, assume the sampling stage performs sampling across the first two modes. Then the outcome of the sampling stage can be represented in the form of a tensor  $\mathcal{Y}$  satisfying

$$\mathcal{Y} = \mathcal{X} \times_1 \mathbf{U}_1 \times_2 \mathbf{U}_2, \quad (3)$$

where  $\mathbf{U}_1 \in \mathbb{R}^{m_r \times N_r}$  and  $\mathbf{U}_2 \in \mathbb{R}^{m_c \times N_c}$ . Here,  $m_r$  and  $m_c$  are the effective number of measurements along the columns and rows, respectively, and  $\mathcal{Y} \in \mathbb{R}^{m_r \times m_c \times N_b}$ . Note that the outcome of the sampling stage is still a tensor of order 3, which indicates that the spatial nature of the data is being preserved; this is in contrast with the method from [5] where the dimensions of the measurement matrix are effectively  $(m_r \cdot m_c) \times N_b$ . Although Eq. 3 can be written in terms of vectorial operations, we use the tensorial representation to highlight the fact that the sampling matrices are of smaller dimensionality than those used in traditional

vectorial approaches; the advantages of the proposed approach are decreased storage and transmission requirements, and, as demonstrated later, reduced computational complexity at the reconstruction stage. Let  $\mathcal{Z}$  denote the samples obtained from sensing the columns of the images, where  $\mathcal{Z} = \mathcal{X} \times_1 \mathbf{U}_1 \in \mathbb{R}^{m_r \times N_c \times N_b}$ . Consequently,  $\mathcal{Y} = \mathcal{Z} \times_2 \mathbf{U}_2$ .

### 3.2. Reconstruction Stage

The reconstruction stage takes the set of samples  $\mathcal{Y}$  as well as the known set of sampling matrices, and reconstructs the color image by solving a set of  $\ell_1$ -minimization tasks. Recovering the original data  $\mathcal{X} \in \mathbb{R}^{N_r \times N_c \times N_b}$  from samples  $\mathcal{Y} \in \mathbb{R}^{m_r \times m_c \times N_b}$  involves reconstruction of the two modes that are compressed in the sampling stage, thus requiring a two-step reconstruction stage. We introduce two alternative approaches to the reconstruction stage, which can be seen as MMV extensions of the tensorial CS recovery stages proposed in [11]. Since the two steps in both approaches are very similar, and for the sake of brevity, we only discuss the first step for each of the approaches in detail. The second step is only briefly summarized at the end of each subsection.

The following discussion applies equally to both approaches. In the first step of the reconstruction stage,  $\mathcal{Y} \in \mathbb{R}^{m_r \times m_c \times N_b}$  together with sampling matrix  $\mathbf{U}_2 \in \mathbb{R}^{m_c \times N_c}$  are used to recover  $\mathcal{Z} \in \mathbb{R}^{m_r \times N_c \times N_b}$ . To this end,  $\mathcal{Y}$  is mode-2 unfolded to obtain  $\mathbf{Y}_{(2)} \in \mathbb{R}^{m_c \times (m_r \cdot N_b)}$ . A matrix  $\mathbf{Z}_{(2)} \in \mathbb{R}^{N_c \times (m_r \cdot N_b)}$  is then formed by stacking solutions  $\mathbf{z}_{(2)i}^* \in \mathbb{R}^{N_c \times 1}$  to the set of  $\ell_1$ -minimization tasks

$$\mathbf{z}_{(2)i}^* = \arg \min \|\mathbf{z}_{(2)i}\|_1 \quad \text{s.t.} \quad \mathbf{y}_{(2)i} = \mathbf{U}_2 \mathbf{z}_{(2)i}, \quad (4)$$

for  $i = 1, 2, \dots, (m_r \cdot N_b)$ ,

where  $\mathbf{y}_{(2)i}$  are the columns of  $\mathbf{Y}_{(2)}$  and  $\mathbf{z}_{(2)i}^*$  are the columns of  $\mathbf{Z}_{(2)}$ . Then  $\mathcal{Z}$  is the tensor whose mode-2 unfolding is  $\mathbf{Z}_{(2)}$ . Note that, as expected,  $\mathcal{Z} \in \mathbb{R}^{m_r \times N_c \times N_b}$ . In the second step,  $\mathcal{Z} \in \mathbb{R}^{m_r \times N_c \times N_b}$  together with sampling matrix  $\mathbf{U}_1 \in \mathbb{R}^{m_r \times N_r}$  are used to recover  $\mathcal{X} \in \mathbb{R}^{N_r \times N_c \times N_b}$  by following the same procedure followed in the first step. We next propose two alternative procedures to solve the above set of  $\ell_1$ -minimization tasks.

#### 3.2.1. Joint recovery across the color dimension

The first procedure to perform the reconstruction step from Eq. 4 exploits the correlation across the color dimension. To that end, the solution to the set of  $\ell_1$ -minimization tasks can be framed as an MMV joint recovery problem as in [5]. Instead of solving the  $m_r \cdot N_b$  minimization tasks from Eq. 4 individually, which would fail to leverage the joint sparsity property across the color dimension,  $m_r$  jointly-sparse matrices of dimensions  $N_c \times N_b$  can be recovered from  $m_r$  measurement matrices of dimensions  $m_c \times N_b$ . Any recovery method for jointly sparse matrices can be employed to achieve this goal. In this paper, we pose this problem as an optimization

task which is effectively the tensorial extension of the method in [1], namely:

$$\mathbf{Z}_{(2)i}^* = [\mathbf{z}_{(2)i1}, \mathbf{z}_{(2)i2}, \dots, \mathbf{z}_{(2)iN_b}] = \arg \min \|\mathbf{Z}_{(2)i}\|_{2,0} \quad \text{s.t.} \\ \mathbf{Y}_{(2)i} = [\mathbf{y}_{(2)i1}, \mathbf{y}_{(2)i2}, \dots, \mathbf{y}_{(2)iN_b}] = \mathbf{U}_2 \mathbf{Z}_{(2)i}, \text{ for } i = 1, 2, \dots, (m_r). \quad (5)$$

The second step of the reconstruction stage which recovers  $\hat{\mathcal{X}}$ , an estimate of  $\mathcal{X}$ , from  $\mathcal{Z}$  and sampling matrix  $\mathbf{U}_1$ , can be carried out in a similar fashion, specifically, by solving  $N_c$  recovery tasks of jointly-sparse matrices of size  $N_r \times N_b$  from  $N_c$  measurement matrices of dimensions  $m_r \times N_b$ .

#### 3.2.2. Joint recovery across the color and spatial dimensions

The second procedure to perform the reconstruction step from Eq. 4 further exploits the correlation across the spatial dimensions. To that end, the solution to Eq. 4 is reduced to a single recovery step of a jointly sparse matrix of size  $N_c \times (m_r \cdot N_b)$  from a single measurement matrix of size  $m_c \times (m_r \cdot N_b)$ . Note that, in this case, joint sparsity across rows and the color dimension is being exploited first. This problem can be expressed as the following optimization task:

$$\mathbf{Z}_{(2)}^* = [\mathbf{z}_{(2)1}, \mathbf{z}_{(2)2}, \dots, \mathbf{z}_{(2)m_r \cdot N_b}] = \arg \min \|\mathbf{Z}_{(2)}\|_{2,0} \quad \text{s.t.} \\ \mathbf{Y}_{(2)} = [\mathbf{y}_{(2)1}, \mathbf{y}_{(2)2}, \dots, \mathbf{y}_{(2)m_r \cdot N_b}] = \mathbf{U}_2 \mathbf{Z}_{(2)}. \quad (6)$$

The second step of the reconstruction stage to recover  $\hat{\mathcal{X}}$ , an estimate of  $\mathcal{X}$ , from  $\mathcal{Z}$  and the sampling matrix  $\mathbf{U}_1$  is carried out in a similar fashion, specifically, by recovering a single jointly-sparse matrix of size  $N_r \times (N_c \cdot N_b)$  from a single measurement matrix of dimensions  $m_r \times (N_c \cdot N_b)$ . This step effectively exploits joint sparsity across columns and the color dimension.

## 4. EXPERIMENTAL RESULTS

In order to verify the efficacy of the proposed methods, we measured their performance both in terms of reconstruction accuracy and execution time. We compare our results to those achieved by the method introduced in [5], which we denote SL2,0, and believe to be state-of-the-art in terms of MMV reconstruction. The legends in the figures in this section refer to the proposed algorithm variant 1 (Sec. 3.2.1) and variant 2 (Sec. 3.2.2) as TMMV1 and TMMV2 respectively, which stand for Tensorial MMV exploiting correlation across the color dimension, and across the color and spatial dimensions.

Reconstruction accuracy was measured in terms of Normalized Mean Squared Error (NMSE) between the reconstructed and original image, and execution time was measured in seconds on a Windows 10 machine with 32GB of RAM and an Intel i7 2.60GHz processor. The implementation of both algorithms was done in Matlab R2016b. Each data point in every figure corresponds to an average of 10 runs. The test RGB image is the commonly used Lena image and is of size  $64 \times 64 \times 3$  pixels. Let  $n = m_r = m_c$  denote the number of measurements along both spatial dimensions of the color

image; the entries of the measurement matrices are drawn from a Gaussian distribution with zero-mean and standard deviation  $\sqrt{\frac{1}{n}}$ . For simplicity, we set the number of measurements for both spatial dimensions to be equal and use the same sampling matrix for both dimensions ( $U_1 = U_2 = U$ ); that is, the randomly constructed Gaussian matrix  $U$  is of size  $n \times 64$  for each mode. Therefore, the measurement matrix for the method in [5] is  $U \otimes U$  of size  $n^2 \times 64^2$ , which results in a total number of measurements of  $3n^2$  across the three color channels. We refer to  $\frac{n^2}{64^2}$  as the normalized number of measurements. We vary the normalized number of measurements from 0.025 to 0.5 in steps of 0.025.

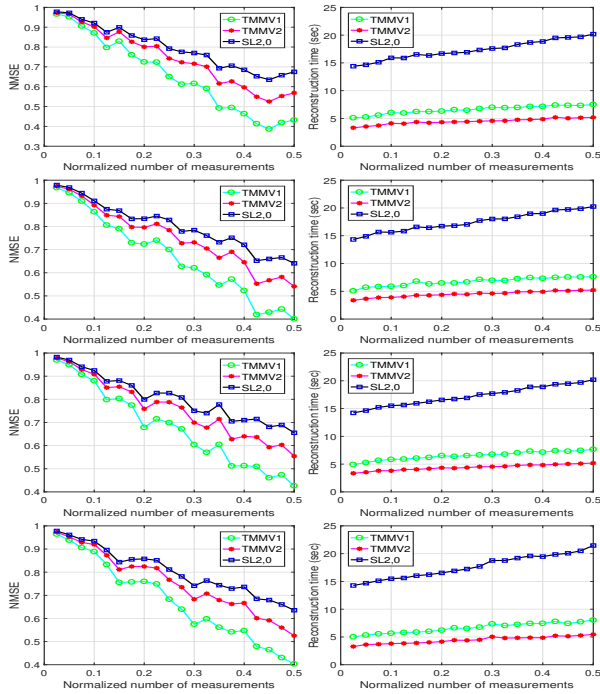


**Fig. 1.** Performance comparison (in terms of reconstruction accuracy - left, and execution times - right) between proposed reconstruction approach and the approach in [5] with row and column sparsity of 10 (row 1), 20 (row 2), 30 (row 3) and 40 (row 4).

Fig. 1 includes reconstruction errors (left column) and execution times (right column) as a function of the normalized number of measurements for all three methods and for different values of column- and row-sparsity (10, 20, 30 and 40 for first, second, third and fourth rows, respectively). The plots on the left column show that TMMV1 and TMMV2 achieve improved reconstruction error since they more effectively exploit correlations in the image while at the same time preserving the spatial structure of the image. We believe TMMV1 slightly outperforms TMMV2 because it is dedicated to exploiting a correlation across a single dimension, as opposed to correlations across two different dimensions, which may be more heterogeneous. However, as discussed next, exploiting spatial and color correlations together leads to a slight gain in computational complexity. The plots on the right column show that TMMV2 is consistently faster than the other two

methods since only a single optimization problem is being solved at each step of the reconstruction stage. Both TMMV1 and TMMV2 are faster than the method from [5] since the measurement matrix for the tensorial approaches has lower dimensionality than its vectorial counterpart. As expected, as the number of measurements being acquired increases, reconstruction error improves at a slight cost of computational complexity. Fig. 2 includes reconstruction errors (left column) and execution times (right column) as a function of different values of column- and row-sparsity for different numbers of normalized measurements (0.025, 0.175, 0.35 and 0.5 for first, second, third and fourth rows, respectively). The results are indicative of similar trends as those observed in Fig. 1. It can also be seen that the degree of sparsity doesn't have a significant effect on the reconstruction error or the execution times.

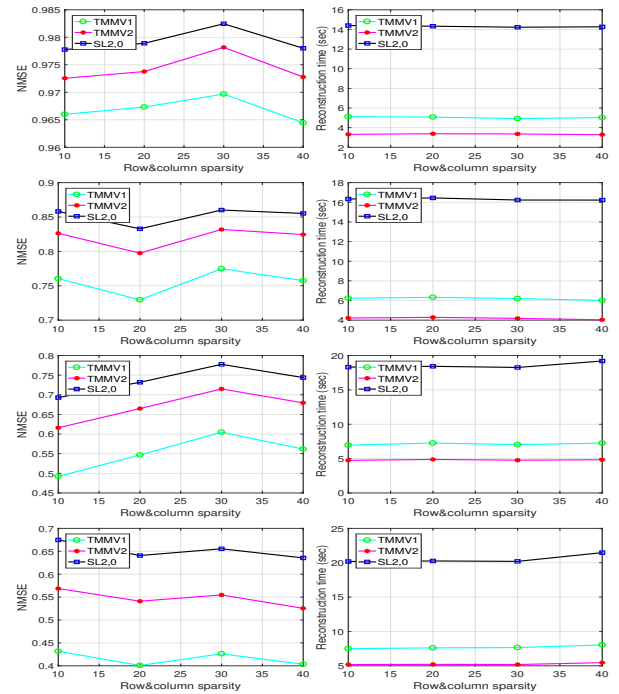


**Fig. 2.** Performance comparison between proposed reconstruction approach and the approach in [5] with the numbers of normalized measurements being fixed to 0.025 (row 1), 0.175 (row 2), 0.35 (row 3) and 0.5 (row 4) respectively.

## 5. CONCLUSION

In this paper, we proposed two different approaches that generalize the MMV framework to support tensorial data. Both methods effectively preserve the tensorial nature of the signals being reconstructed, while at the same time exploiting correlations across the color and/or the spatial dimensions. We empirically demonstrated the superior performance of both of the methods relative to the state-of-the-art with regards to reconstruction accuracy and execution times. While exploiting correlations only across the color dimension results in better reconstruction quality, simultaneously leveraging correlations across the color and spatial dimensions results in computational advantages.

## 6. REFERENCES

- [1] J. Chen and X. Huo, "Theoretical results on sparse representations of multiple-measurement vectors," *IEEE Transactions on Signal Processing*, vol. 54, no. 12, pp. 4634–4643, Dec 2006.
- [2] S. F. Cotter, B. D. Rao, Kjersti Engan, and K. Kreutz-Delgado, "Sparse solutions to linear inverse problems with multiple measurement vectors," *IEEE Transactions on Signal Processing*, vol. 53, no. 7, pp. 2477–2488, July 2005.
- [3] E. van den Berg and M. P. Friedlander, "Theoretical and empirical results for recovery from multiple measurements," *IEEE Transactions on Information Theory*, vol. 56, no. 5, pp. 2516–2527, May 2010.
- [4] M. Mishali and Y. C. Eldar, "Reduce and boost: Recovering arbitrary sets of jointly sparse vectors," *IEEE Transactions on Signal Processing*, vol. 56, no. 10, pp. 4692–4702, Oct 2008.
- [5] A. Majumdar, R. K. Ward, and T. Aboulnasr, "Algorithms to approximately solve np hard row-sparse mmv recovery problem: Application to compressive color imaging," *IEEE Journal on Emerging and Selected Topics in Circuits and Systems*, vol. 2, no. 3, pp. 362–369, Sept 2012.
- [6] A. Majumdar and R. K. Ward, "Compressive color imaging with group-sparsity on analysis prior," in *2010 IEEE International Conference on Image Processing*, Sept 2010, pp. 1337–1340.
- [7] G. Hennenfent, E. van den Berg, M. P. Friedlander, and F. J. Herrmann, "New insights into one-norm solvers from the pareto curve," *GEOPHYSICS*, vol. 73, no. 4, pp. A23–A26, 2008.
- [8] A. Gogna, A. Shukla, H. K. Agarwal, and A. Majumdar, "Split bregman algorithms for sparse / joint-sparse and low-rank signal recovery: Application in compressive hyperspectral imaging," in *2014 IEEE International Conference on Image Processing (ICIP)*, Oct 2014, pp. 1302–1306.
- [9] K. Chang, Y. Liang, C. Chen, Z. Tang, and T. Qin, "Color image compressive sensing reconstruction by using inter-channel correlation," in *2016 Visual Communications and Image Processing (VCIP)*, Nov 2016, pp. 1–4.
- [10] E. A. Bernal and Q. Li, "Hybrid vectorial and tensorial compressive sensing for hyperspectral imaging," in *2015 IEEE International Conference on Acoustics, Speech and Signal Processing (ICASSP)*, April 2015, pp. 2454–2458.
- [11] S. Friedland, Q. Li, D. Schonfeld, and E. A. Bernal, "Two algorithms for compressed sensing of sparse tensors," *CoRR*, vol. abs/1404.1506, 2014.
- [12] X. Ding, W. Chen, and I. Wassell, "Nonconvex compressive sensing reconstruction for tensor using structures in modes," in *2016 IEEE International Conference on Acoustics, Speech and Signal Processing (ICASSP)*, March 2016, pp. 4658–4662.
- [13] Q. Li and E. A. Bernal, "Hybrid tensor-vectorial compressive sensing for hyperspectral imaging," *Journal of Electronic Imaging*, vol. 25, no. 3, pp. 033001, 2016.